Opposite phase changes of precipitation annual cycle over land and ocean under global warming

Fengfei Song[1], Jian Lu[1], L. Ruby Leung[1], Fukai Liu[2]

1. Atmospheric Sciences and Global Change Division, Pacific Northwest National Laboratory, Richland, Washington, USA

2. Physical Oceanography Laboratory/CIMST, Ocean University of China and Qingdao National Laboratory for Marine Science and Technology, Qingdao, China

Supplementary information:

One table and 6 Figures.

Submitted to *Geophysical Research Letters*

Corresponding authors:

Jian Lu (jian.lu@pnnl.gov) and L. Ruby Leung (ruby.leung@pnnl.gov)

20 **Supplementary Table 1** Data from the HIST and RCP85 simulations in 37 CMIP5 models used

21 in this study.

No.	Model	Energy fluxes	Other variables
1	ACCESS1-0	×	×
2	ACCESS1-3	×	×
3	bcc-csm1-1	×	×
4	bcc-csm1-1-m	×	×
5	BNU-ESM	×	×
6	CanESM2	×	×
7	CCSM4	×	×
8	CESM1-BGC	×	×
9	CESM1-CAM5	×	×
10	CESM1-WACCM	×	×
11	CMCC-CESM	×	×
12	CMCC-CM	×	×
13	CMCC-CMS	×	×
14	CNRM-CM5	×	×
15	CSIRO-Mk3-6-0	×	×
16	FGOALS-g2	×	×
17	FIO-ESM		×
18	GFDL-CM3	×	×
19	GFDL-ESM2G	×	×
20	GFDL-ESM2M	×	×
21	GISS-E2-H	×	×
22	GISS-E2-R	×	×
23	HadGEM2-AO		×
24	HadGEM2-CC	×	×
25	HadGEM2-ES	×	×
26	inmcm4	×	×
27	IPSL-CM5A-LR	×	×
28	IPSL-CM5A-MR	×	×
29	IPSL-CM5B-LR	×	×

30	MIROC5	×	×
31	MIROC-ESM-CHEM	×	×
32	MIROC-ESM	×	×
33	MPI-ESM-LR	×	×
34	MPI-ESM-MR	×	×
35	MRI-CGCM3	×	×
36	NorESM1-M	×	×
37	NorESM1-ME	×	×

22

Correlation = 0.94 (NH: 0.97; SH: 0.89)   RCP85 - HIST
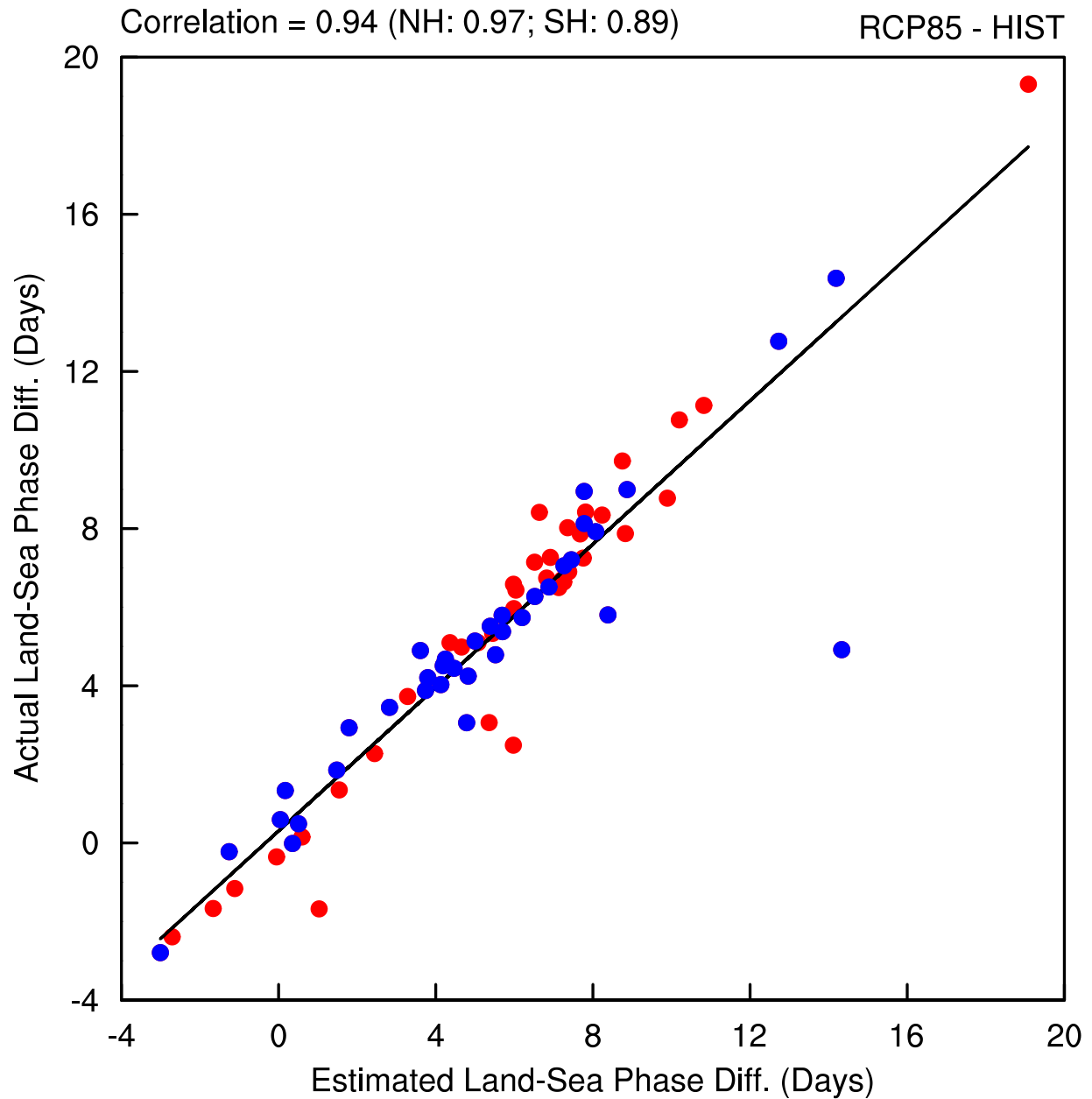
Supplementary Fig. 1 Scatterplot between the change of the actual land-sea phase difference and the corresponding estimate (i.e., $\phi_L - \phi_O$) among the CMIP5 models in NH (red dots) and SH (blue dots). Each dot represents one model. Positive value indicates that land and ocean precipitation become more in phase with each other. The correlation is 0.97 in NH and 0.89 in SH, respectively.
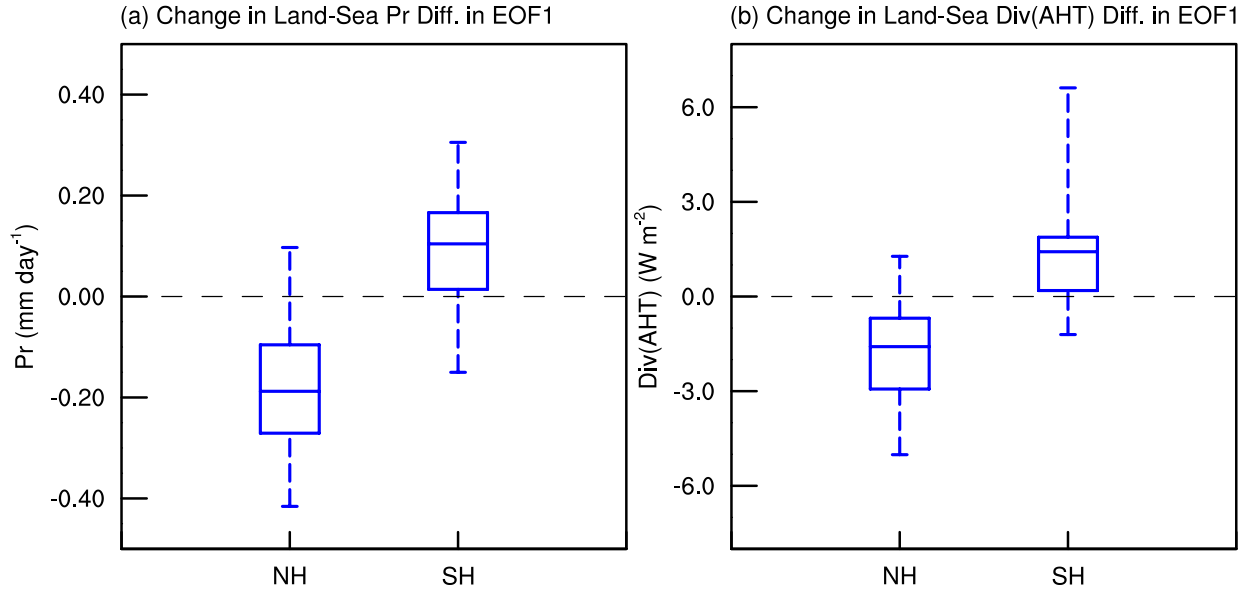
Supplementary Fig. 2 Box-plots for the change (RCP85 – HIST) in land-sea difference of (a) precipitation (unit: mm day^{-1}) and (b) divergence of atmospheric heat transport ($\nabla \cdot (AHT)$; unit: W m^{-2}) regressed on the precipitation EOF1 among CMIP5 models.

33
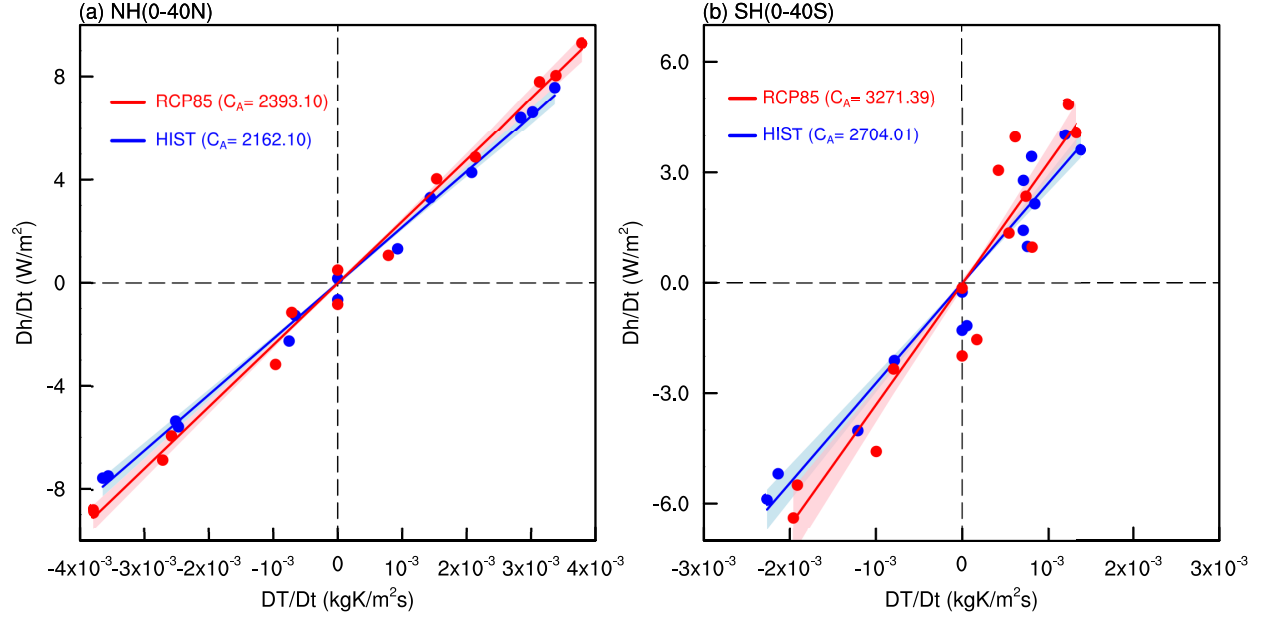
Supplementary Fig. 3 Scatterplot and regression between the monthly tendencies of $\langle h \rangle$ and $\langle T \rangle$. These tendencies are computed based on the multi-model ensemble mean climatological monthly values averaged over (a) NH (0°-40°N) and (b) SH (0°-40°S), respectively. The regression slope (C_A) provides an estimate of the effective atmospheric heat capacity in the hemisphere examined. The blue and red dots and lines are for the HIST and RCP85 simulations, respectively. The shading indicates one standard deviation of the regression slope among the CMIP5 models.

40
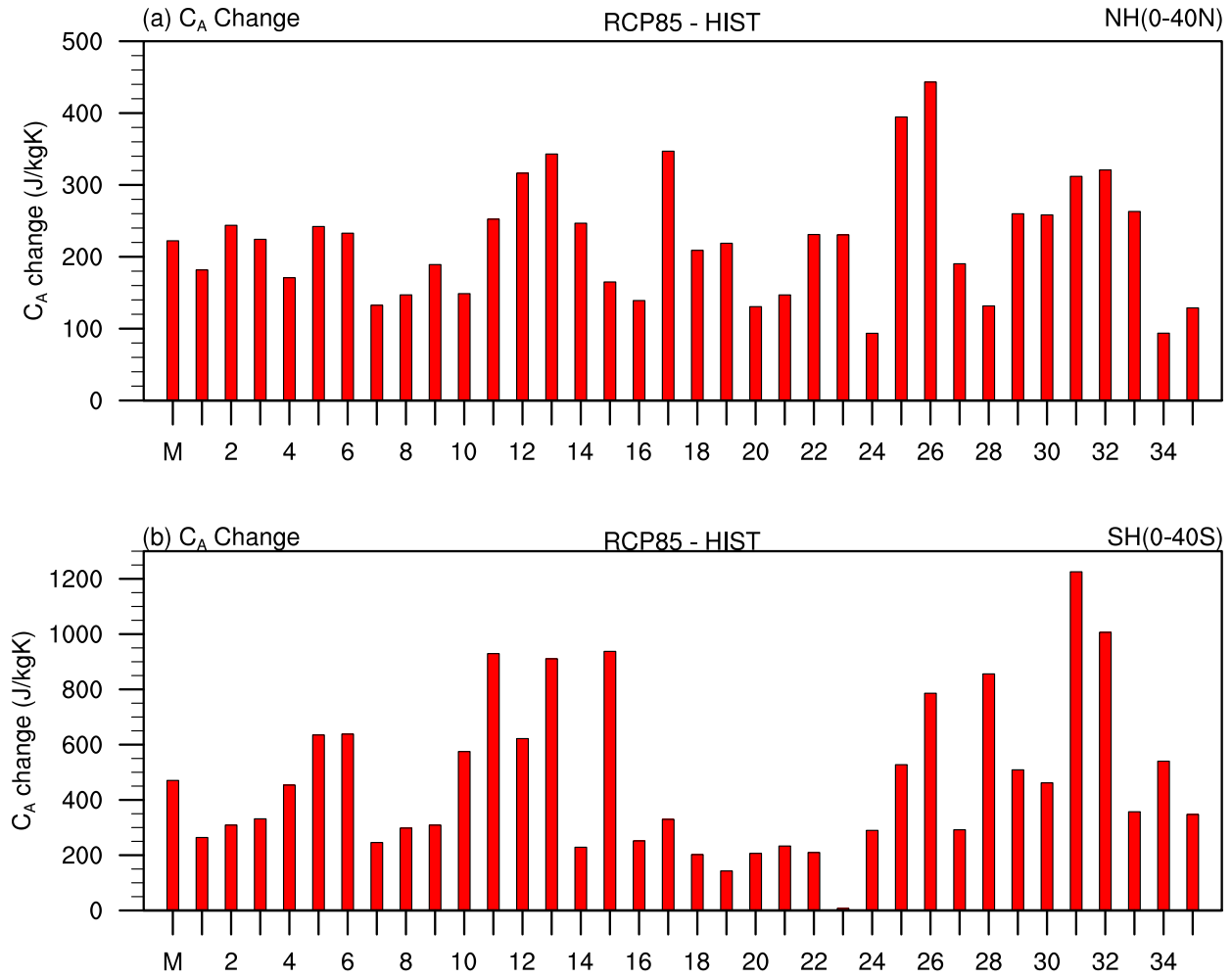
Supplementary Fig. 4 The effective atmospheric heat capacity C_A changes between the RCP85

and HIST experiments in the CMIP5 models in (a) NH (0°-40°N) and (b) SH (0°-40°S). M

indicates the multi-model ensemble mean and each number denotes one of the 35 CMIP5 models.

(a) Beta   HIST

(b) Beta   RCP85 - HIST

44
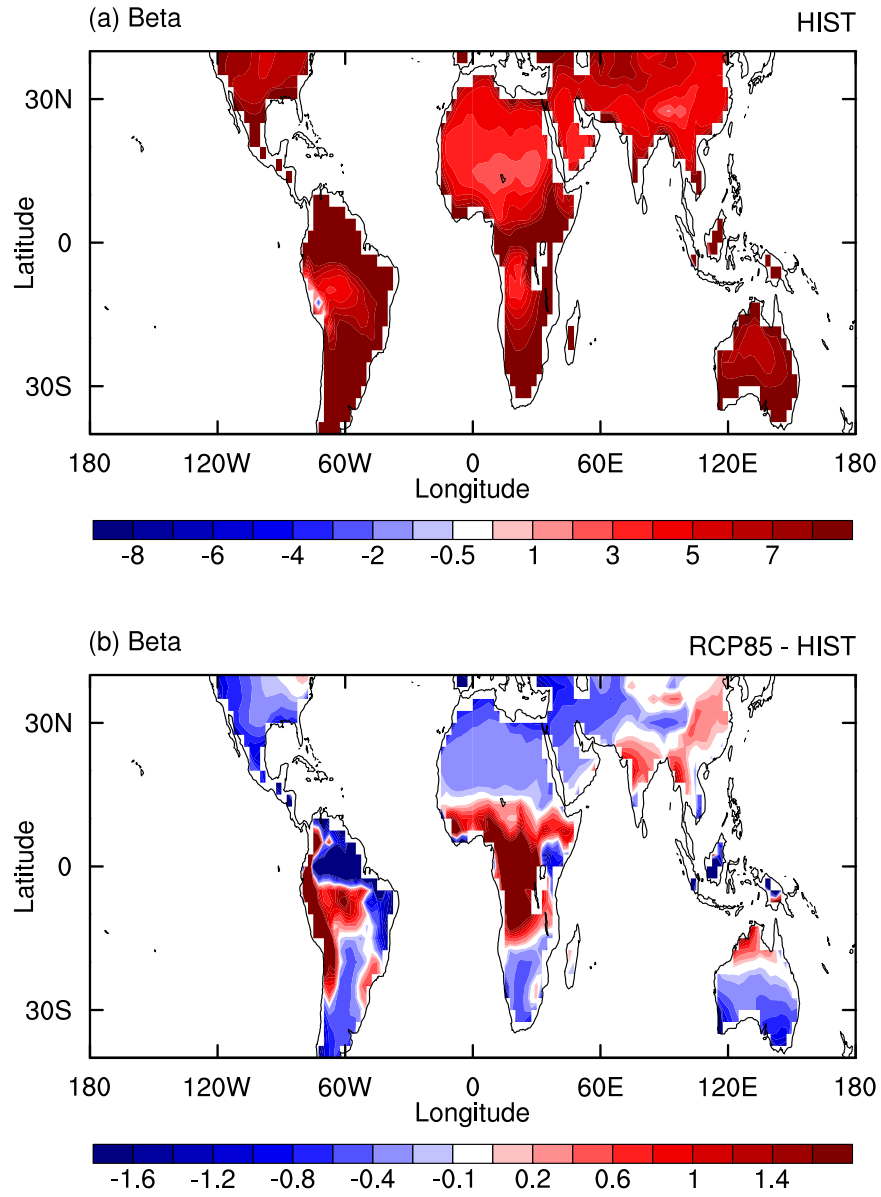
Supplementary Fig. 5 The surface cooling feedback parameter β in (a) the HIST run and (b) its

change between the RCP85 and HIST runs.
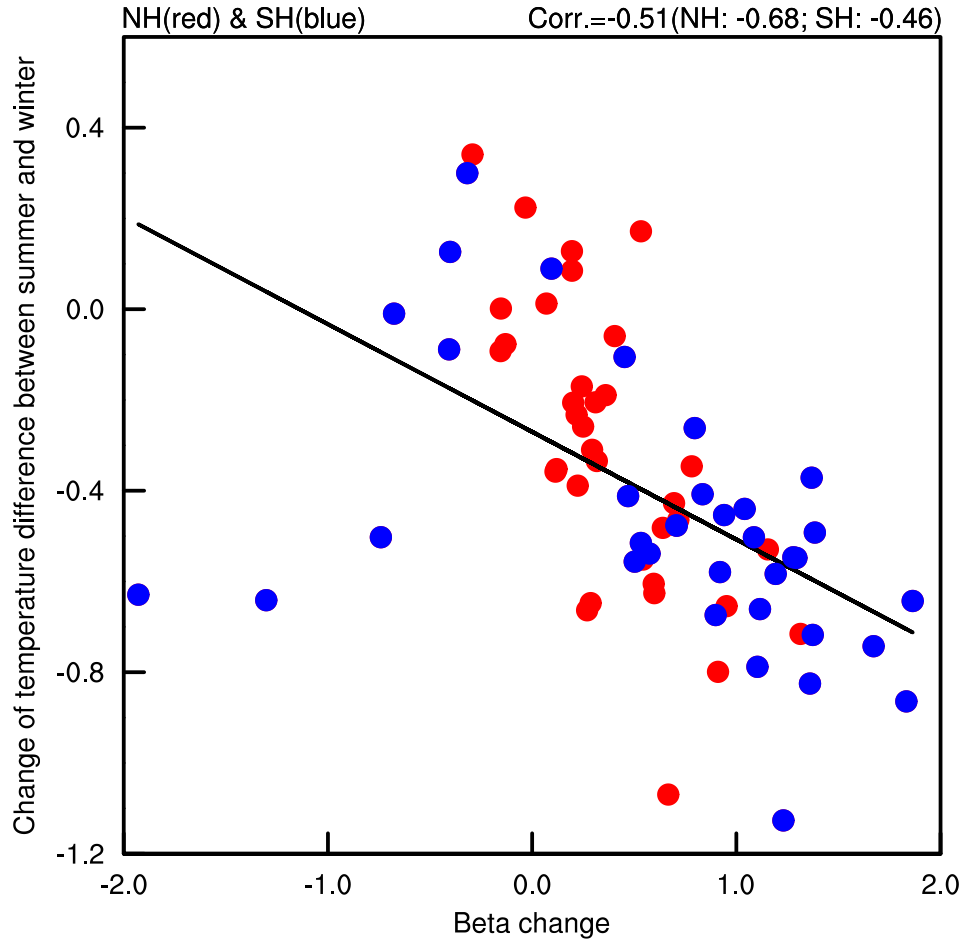
Supplementary Fig. 6 Scatterplot between the change of surface cooling feedback β and the temperature difference between summer (July-August-September (JAS) for NH and January-February-March (JFM) for SH) and winter (JFM for NH and JAS for SH) over the land monsoonal regions, which are defined as regions with the magnitude of precipitation anomalies in EOF1 greater than 0.5 mm day^{-1}. Each dot represents one CMIP5 model with red (blue) for NH (SH). The correlations are listed at the upper-right corner of the figure, all being statistically significant at 1% level based on Student's t-test. Note that the correlation for SH can be augmented to -0.81 when three outlier models (GFDL-ESM2G, GFDL-ESM2M and GISS-E2-H) are excluded.